Proceedings of the 2nd International Conference on Mathematical Physics and Computational Simulation
DOI: 10.54254/2753-8818/36/20240535

Design and simulation implementation of bismuth-doped fiber laser

Yufei Chen

School of physics, Donghua University, Shanghai, China

211410115@mail.dhu.edu.cn

Abstract. Rare-earth doped fibers are an important means of expanding the wavelength band of optical fibers. Currently, researchers aim to broaden the working wavelength band of optical fibers by doping with different rare-earth elements, thereby increasing the amount of information that can be transmitted. In this paper, a bismuth-doped fiber laser operating around 1300nm was designed. A basic physical model for implementing a bismuth-doped fiber laser was proposed based on the energy levels and transition processes of bismuth, rate, and power propagation equations. It was possible to determine the link between pump power and laser power at a wavelength of 1300 nm by modeling tests using the physical model. Additionally, the relationship between pump light and laser power in bismuth-doped fiber at different positions and propagation directions was analyzed. Suggestions for the future large-scale application of bismuth-doped fiber lasers around the 1300nm wavelength band were provided.

Keywords: Bismuth-doped fiber laser, amplified spontaneous emission, power propagation equation

1. Introduction

Lasers, with characteristics such as high brightness, monochromaticity, coherence, and good directionality, have been widely used in scientific research, communication, military, industrial, medical, and other fields. With the rapid development of applications such as the internet, 5G, and cloud storage, the global annual information communication volume has surged. Fiber optics communication has become a crucial means of information transmission. Improving information transfer rates is mainly achieved by increasing data transmission and demodulation speeds and expanding the system's transmission bandwidth. Quartz fiber covers the available bandwidth in the range of 1250-1800nm, and by doping fibers with rare earth elements, different spectral bands can be covered to widen the transmission bandwidth [1]. Existing fiber lasers, such erbium-doped fiber amplifiers, only work well in the 1530–1610 nm range, and there are no fiber amplifiers for other wavelengths [2].

The major method used to manufacture erbium-doped fibers is an enhanced chemical vapor deposition procedure in conjunction with solution doping methods [3]. Multiple spatial transmission modes may be supported by these fibers by adjusting parameters including refractive index profile, doping concentration, and core diameter.. In 2011, the University of Southampton in the UK first drew a dual-mode erbium-doped fiber, supporting two modes, and achieved gains of over 20 dB in the 1550-1560 nm range using 980 nm laser pumping. Subsequently, various types of dual-mode erbium-doped fibers have emerged, focusing on aspects such as fabrication processes, number of transmission modes,

DOI: 10.54254/2753-8818/36/20240535

operating wavelengths, gains, differential mode gains, noise, and more [4]. Using dual-mode fibers as transmission lines in space division multiplexing technology requires long-distance transmission, making dual-mode erbium-doped fiber amplifiers crucial devices for compensating for fiber transmission losses [5]. However, in dual-mode erbium-doped fiber amplifiers, high differential mode gain can increase the probability of system interruptions, affecting signal quality [6].

Bismuth, unlike common rare earth elements, has an electron configuration of $4f^{14}5d^{10}6s^{2}6p^{3}$. The inner subshell of bismuth is filled, and the outer 6s and 6p electrons can undergo significant chemical reactions with the host glass components. Therefore, bismuth exhibits emission and absorption characteristics depending on the host material [7]. The oxidation states of multivalent bismuth include Bi^{+}, Bi^{2+}, Bi^{3+}, and Bi^{5+}. It is crucial to produce the desired oxidation states in a controlled manner when manufacturing fibers and optical preforms. It is widely believed that when high oxidation states are reduced to low oxidation states, near-infrared fluorescence is produced. However, the preparation process of bismuth-doped fibers depends on various factors such as temperature, pressure, and concentrations of different components, making it challenging to control the oxidation-reduction equilibrium to the appropriate state. Excessive high-valence bismuth ions being reduced and producing bismuth oligomers and metal colloids can lead to a decrease in near-infrared emission centers [8-10]. Regardless of theory and research, there is still controversy over the origin and specific reasons for near-infrared emission centers in bismuth. To boost the efficiency of systems and the performance of bismuth-doped fiber materials, a more thorough investigation into the near-infrared emission characteristics of these fibers is required. Bismuth-doped, Bi/Er co-doped, and quantum dot-doped glasses and fibers can produce ultra-wideband fluorescence covering 1050-1800nm, making them potential gain media for ultra-wideband or even full-band fiber lasers. This widens the utilization of quartz fibers in low-loss communication and expands transmission bandwidth [2,11,12].

In this paper, bismuth-doped fibers are selected as the gain medium. Using a theoretical physics model and numerical simulation methods, a fiber laser working around 1310nm wavelength is designed with laser pumping near 808nm wavelength. This design aims to provide a possibility for the subsequent expansion of fiber working ranges for applications and research in the 1300-1350nm range.

2. Theoretical Model

Bi atoms have an outermost electron configuration of $4f^{14}5d^{10}6s^{2}6p^{3}$. The ground state energy level of Bi ions is 3P0, therefore, absorption spectral lines occur at 0.5μm, 0.7μm, 0.8μm, and 1.0μm when electrons transition from $3p^{0}$ to $1S^{0}$, $3P^{0}$ to $1D^{2}$, $3P^{0}$ to $1P^{2}$, and $3P^{0}$ to $1P^{1}$, respectively [13]. Thus, a three-level system is used to describe the transition process as shown in Figure 1. Utilizing an 808nm pump light source, electrons are excited to the $3P^{2}$ level. Particles on the $3P^{0}$ level undergo spontaneous emission transition to the $3P^{1}$ level, while some particles on the $3P^{2}$ level undergo non-radiative transition to the $3P^{1}$ level. Particles on the $3P^{1}$ level then undergo stimulated emission and non-radiative transitions back to the first level [14].W_P represents the pump light absorption rate, W_{12} is the signal light absorption rate, W_{21} is the stimulated emission rate of the signal light, A_{32} is the non-radiative transition rate, and A_{21} is the radiative transition rate.

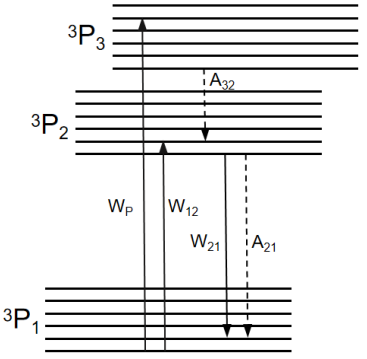

Figure 1. Schematic diagram of the transition between three energy levels of Bi

DOI: 10.54254/2753-8818/36/20240535

In Fig. 1, The transition rate equations for the electron between the three energy levels can be obtained as follows:

$$\frac{\partial N_1(z)}{\partial t} = -[W_p(z) + W_{12}(z)]N_1(z) + A_{21}N_2(z) + W_{21}(z)N_2(z)) \quad (1)$$

$$\frac{\partial N_2(z)}{\partial t} = W_{12}(z)N_1(z) - W_{21}(z)N_2(z) - A_{21}N_2(z) + A_{32}N_3(z) \quad (2)$$

$$\frac{\partial N_3(z)}{\partial t} = W_p(z)N_1(z) - A_{32}N_3(z) \quad (3)$$

$$N = N_1(z) + N_2(z) + N_3(z) \quad (4)$$

Where $W_p(z) = \frac{\sigma_{13}P_p(z)}{ln_{13}\ A_{eff}}$, $W_{12}(z) = \frac{\sigma_{12}(v_{12})(z)}{ln_{12}\ A_{eff}}$, $W_{21}(z) = \frac{\sigma_{21}(v_{21})(z)}{ln\ n_{21}A_{eff}}$, $A_{eff} = \pi r^2$.

Where the following are represented in units of per second (/s): $W_p(z)$, $W_{12}(z)$, $W_{21}(z)$, $A_{32}(z)$, $A_{21}(z)$ denote the pump light absorption rate, signal light absorption rate, stimulated emission rate of signal light, non-radiative transition rate, and radiative transition rate, respectively. r is the radius of the optical fiber core. P_P and P_S denote the pump power and stimulated emission power, respectively. The cross-sections for pump light absorption, signal light absorption, and signal light emission are σ_{13}, σ_{12}, and σ_{21} respectively. The optical fiber's cross-sectional area is denoted by A_{eff}. Fig. 2 depicts the propagation of laser and pump light power in the optical fiber.

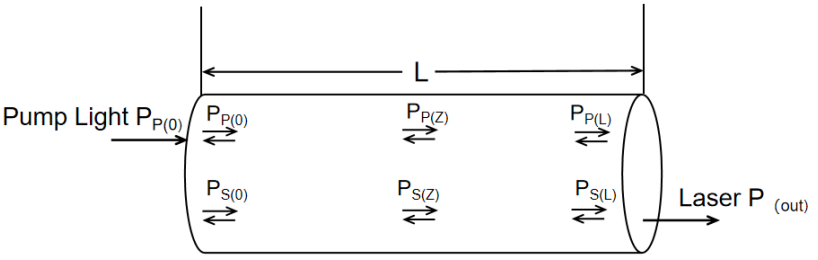

Figure 2. Diagrammatic representation of how laser and pump light powers propagate across optical fibers

From Fig. 2, the propagation equations for laser power and pump light in bismuth-doped optical fiber may be obtained as follows.

$$\frac{dP_p^+(z)}{dz} = \Gamma_p(-\sigma_{13}N_1(z) - \alpha_p)\,(z) \quad (5)$$

$$\frac{dP_p^-(z)}{dz} = -\Gamma_p(-\sigma_{13}N_1(z) - \alpha_p)\,(z) \quad (6)$$

$$\frac{dP_s^+(z)}{dz} = \Gamma_s[\sigma_{21}N_2(z) - \sigma_{12}N_1(z) - \alpha_s]\,(z) \quad (7)$$

$$\frac{dP_s^-(z)}{dz} = -\Gamma_s[\sigma_{21}N_2(z) - \sigma_{12}N_1(z) - \alpha_s]\,(z) \quad (8)$$

3. Design and Simulation Experiment of Laser

Design a single-end pump-pumped bismuth-doped fiber laser for the simulation experiment model. LDs are fiber-coupled semiconductor lasers providing pump light to the laser. Lower-power pump light is combined with higher-power pump light using a beam combiner and injected into the bismuth-doped fiber. The fiber doped with bismuth exhibits a high reflectivity. Bragg grating and a fiber with low reflectance Pump light and laser are able to oscillate back and forth in the fiber due to the bragg grating on both ends. The laser emitted from the bismuth-doped fiber passes through a cladding light stripper

DOI: 10.54254/2753-8818/36/20240535

and is then transmitted through a delivery fiber to the fiber optic connector. Finally, it is collimated and output from the fiber optic connector.

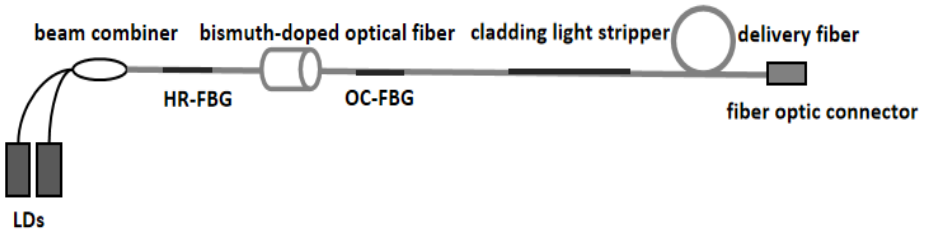

Figure 3. Design structure diagram of bismuth-doped fiber laser

Here is the simulated experimental data based on [13,14], presented in the following Table 1.

Table 1. Experimental parameters in the rate equation and power propagation equation

Symbol	Physical Parameter	Numerical Value	Unit
λ_{sp}	Pump light central wavelength	$8.08*10^{-7}$	m
λ_s	Fiber laser central wavelength	$1.3*10^{-6}$	m
τ	Bismuth ion average level lifetime	$5*10^{-4}$	s
σ_{13}	Pump light absorption cross-section	$1.3*10^{-28}$	m^2
σ_{31}	Pump light emission cross-section	$2*10^{-29}$	m^2
σ_{12}	Stimulated emission absorption cross-section	$1*10^{-28}$	m^2
σ_{21}	Stimulated emission emission cross-section	$1*10^{-28}$	m^2
A_{eff}	Core cross-sectional area	$2*10^{-11}$	m^2
N	Number of bismuth ions in the core	$1.8*10^{24}$	count
α_p	Dual-clad fiber loss for pump light	$2*10^{-3}$	m^{-1}
α_s	Dual-clad fiber loss for laser light	$4*10^{-4}$	m^{-1}
L	Dual-clad fiber length	1	m
Γ_p	Pump light power fill factor	0.82	/
Γ_s	Laser power fill factor	0.74	/
R_1	Left boundary mirror reflectivity	0.99	/
R_2	Right boundary mirror reflectivity	0.635	/

By substituting the above parameters into the model and performing numerical simulations in Matlab, Fig. 4 and Fig. 5 are obtained.

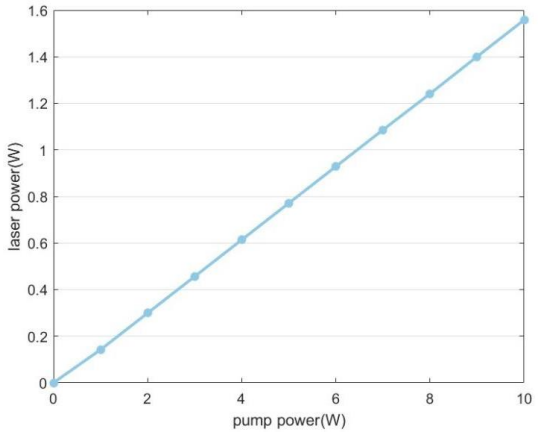

Figure 4. The connection between pump power and laser power

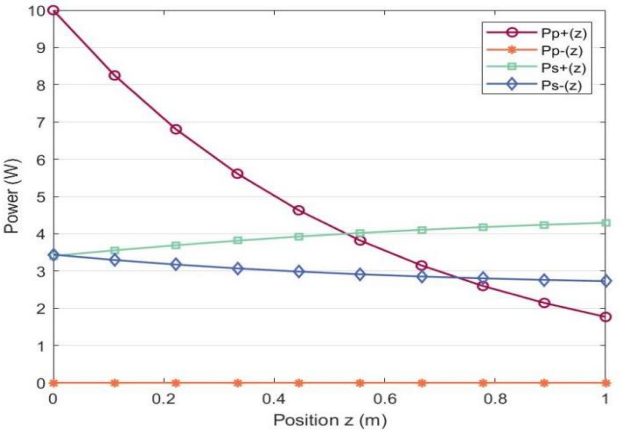

Figure 5. Pump power and laser power relationship as a function of location

DOI: 10.54254/2753-8818/36/20240535

Based on the analysis of Fig. 4 by taking data points, we find that the laser power increases nonlinearly with increasing pump power. At a pump power of 3W, the laser power is found to be 0.4563W. Additionally, from Fig. 5,it is possible to acquire the strength of the laser and pump light at various points along the forward and reverse propagation paths. It can also be observed from the figure that when the pump light propagates forward to the right boundary, there is still a power of approximately 1.9W, which means that increasing the length of the laser can lead to greater laser power.

4. Conclusion

In conclusion, this paper presents the energy levels and structure of electron transitions in bismuth-doped fiber, the physical model, and simulation results. From the simulation results, it is evident that within a certain range, the larger the pump power of the bismuth-doped fiber laser, the greater the output laser power. Additionally, in this simulation experiment, a bismuth-doped fiber length of 1m was used. However, it was found at the right boundary that nearly 1/5 of the pump power was not consumed. This suggests that increasing the fiber length could enhance the consumption rate of pump power. It is crucial to identify a relatively short fiber length where the majority of the pump power is used in order to increase the laser system's efficiency and save expenses. This lays the foundation for future large-scale applications of bismuth-doped fiber in the vicinity of the 1300nm wavelength band. Bismuth-doped fiber is also becoming an important material for expanding the range of fiber wavelengths, even forming a laser gain medium for the entire wavelength range. The bismuth-doped laser created in this study operates in the 1300 nm wavelength range. Based on the properties of bismuth-doped fiber, lasers for additional wavelength bands may be built in the future.

References

[1] Ghatak K 1998 An introduction to fiber optics CUP
[2] Yevgeny D 2020 Development and prospects of bismuth-doped optical fibers Opt Laser Technol vol 18 no 1 pp 1-4
[3] Bufetovr A Melkumov A 2014 Bi-Doped Optical Fibers and Fiber Lasers J Sel Top Quant
[4] Murata K Fujimoto T 1999 Bi-doped SiO 2 as a new laser material for an intense laser Fusion Eng Des vol 1
[5] Yasushi F Masahiro N 2003 Optical amplification in bismuth-doped silica glass Appl Phys Lett
[6] Peng M Qiu J 2004 Bismuth- and aluminum-codoped germanium oxide glasses for super-broadband optical amplification Opt Lett
[7] Lobach A 2016 Narrowband random lasing in a Bismuth-doped active fiber Sci Rep vol 6 no1
[8] Khonthon S 2007 Luminescence characteristics of Te-and Bi-doped glasses and glass-ceramics J Ceram Soc pp 259-263
[9] Sokolov V Plotnichenko G 2008 Origin of broadband near-infrared luminescence in bismuth-doped glasses Opt. Lett vol 33 no 13 pp 1488-1490.
[10] Dianov E M 2015 Nature of Bi-related near IR active centers in glasses: state of the art and first reliable results Laser Phys Lett vol 12 no 9
[11] Donodin A 2022 Bismuth-doped fibre amplifiers for multi-band optical networks Diss Aston Uni
[12] Dianov E M 2012 Bismuth-doped optical fibers: a challenging active medium for near-IR lasers and optical amplifiers Light Sci Appl vol 1 no 5
[13] Jiang Ch 2009 Modeling a broadband bismuth-doped fiber amplifier J Sel Top Quantum Electron vol 15 no 1 pp 79-84
[14] Meng X 2005 Near infrared broadband emission of bismuth-doped aluminophosphate glass Opt Express vol 13no 5 pp 1628-1634